

Status of the SWGO air shower reconstruction using a template-based likelihood method

F. Leitl,^{a,*} V. Joshi^a and S. Funk^a for the SWGO Collaboration

^a*Friedrich-Alexander-Universität Erlangen-Nürnberg, Erlangen Centre for Astroparticle Physics
Nikolaus-Fiebiger-Str. 2, D 91058 Erlangen, Germany*

E-mail: franziska.leitl@fau.de

The Southern Wide-field Gamma-ray Observatory (SWGO) is a proposed facility for ground-based gamma-ray astronomy. It will consist of an array of water Cherenkov detectors to detect astrophysical gamma-rays mainly in the range of hundreds of GeV up to the PeV scale. To be constructed in South America, it will feature an approximately two-steradian field of view and a duty cycle close to 100%, which will complement the current generation of instruments by extending survey coverage to the Southern Hemisphere. As part of the development of the SWGO standard reconstruction framework, we employ a Monte Carlo template-based method to estimate the properties of the primary gamma-ray (such as core position and energy). In this method, an observed lateral amplitude distribution of a gamma-ray-induced air shower is fitted to the expected probability distribution stored in the templates. We validate this approach by estimating the energy performance for one of the currently investigated test array and detector unit configurations for SWGO.

38th International Cosmic Ray Conference (ICRC2023)
26 July - 3 August, 2023
Nagoya, Japan



*Speaker

1. Introduction

In the last decade, various experimental techniques for the precise measurement of astrophysical gamma rays have been established. Direct detection methods usually investigate gamma rays in a lower energy range, like for example, the Large Area Telescope (Fermi/LAT) that covers an energy range of a few MeV to some hundreds of GeV [1]. Ground-based instruments are used at higher energies since the particle flux becomes too small to be detected directly [2].

At these energies, impinging gamma rays interact with the nuclei in the atmosphere and generate particle showers made up of mostly secondary electrons, positrons, and photons. Once these secondary particles enter a detection unit that is filled with water, they produce Cherenkov radiation [3] that can be observed with photomultiplier tubes (PMTs). The deposited signal and timing measured in the detection units can be used for the shower reconstruction to estimate important characteristics of the primary gamma ray, such as the energy or direction of the particle. Current gamma-ray experiments that apply the water Cherenkov detection technique include the High-Altitude Water Cherenkov (HAWC) Observatory which is located in Mexico [4] and the Large High Altitude Air Shower Observatory (LHAASO) in China [5]. So far, experiments of this type are limited to the Northern Hemisphere.

The Southern Wide-field Gamma-ray Observatory (SWGO) is a future instrument for ground-based gamma-ray astronomy that will also use water Cherenkov detection. It is planned to be constructed in South America and extend current-generation instruments to the Southern Hemisphere. It will allow an approximately two-steradian field of view and a duty cycle close to 100% and primarily study gamma rays in an energy range of hundreds of GeV up to the PeV scale¹ [6]. To get information about the energy, direction, and core position of those gamma rays, their initiated particle cascades have to be reconstructed.

In this work, we describe the standard reconstruction method to reconstruct the energy and core position for gamma-induced particle showers for SWGO, which is currently being developed.

2. Template-based reconstruction method

Based on the success of template-based reconstruction strategies in other experiments, such as HAWC [7], we adapted the algorithm to the design of SWGO. An important advantage of the template-based technique is that the signal measured in the detection units can be incorporated directly in the reconstruction when filling the templates and does not have to be approximated [7]. This enables a stable reconstruction suffering from fewer fluctuations.

While the final layout of SWGO is not finalized, a few test configurations are available that are currently being investigated [8]. For this work, we used one of the currently available test array layouts. An image of the array layout can be found in Figure 1. The detection units consist of double-layered cylindrical tanks. Each cell includes one PMT. The PMT in the upper cell is fixed at the bottom of the cell, while the PMT in the lower cell is mounted to the top. The tanks have a diameter of 3.82 m, the upper cell has a height of 2.5 m, and the lower cell of 0.5 m, respectively. In this analysis, we limited ourselves to the use of the upper cells for the reconstruction. The array consists of two zones, a dense inner zone, and a sparser outer zone. The radius of the inner zone is

¹Updated information on the official SWGO website <https://www.swgo.org/SWGWiki/doku.php>.

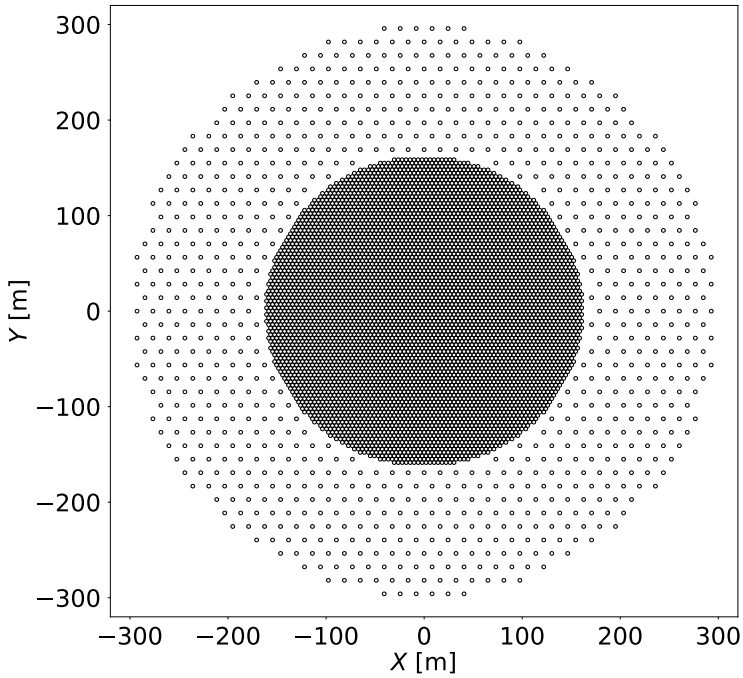


Figure 1: Test array layout of SWGO with a dense inner zone where the tank units stand wall to wall and a sparser outer zone.

	Bin range	Bin size
$\log_{10}(E)$	1.5 – 6.0	0.05
X_{\max}	150 g/cm ² – 750 g/cm ²	50 g/cm ²
θ	0° – 50°	0.06 in $\cos(\theta)$

Table 1: Binning of the simulated gamma-induced air showers that were used to fill the templates.

160 m where the tanks are positioned so that their walls touch the neighboring tanks. The radius of the outer zone is 300 m. The array is simulated at a height of 4.7 km above sea level.

We used simulations of gamma-induced air showers in an energy range of a few tens of GeV up to 1 PeV that were thrown in a radius of 1.5 km around the array center. The first interaction of the primary gamma ray as well as the shower development in the atmosphere was simulated with CORSIKA (version 7.740) [9]. The interaction of the secondary particles with the water tanks was simulated with GEANT4 (version geant4-10-00-patch-04) [10].

The simulated showers that are used to fill the templates are binned in energy E , maximum shower depth X_{\max} and zenith angle θ (see Table 1). Both the information of a single tank that measured charge as well as the information that no signal was measured are used. After filling the templates, we applied a smoothing using a Gaussian distributed weighted sum. An example of a smoothed template is shown in Figure 2.

The 2D histogram of Figure 2 shows the probability distribution of measuring a certain number of photoelectrons (N_{pe}) at a particular distance r between each tank and the shower core in the shower plane. Note that N_{pe} is a decimal number since it is processed with a jitter to represent the jitter

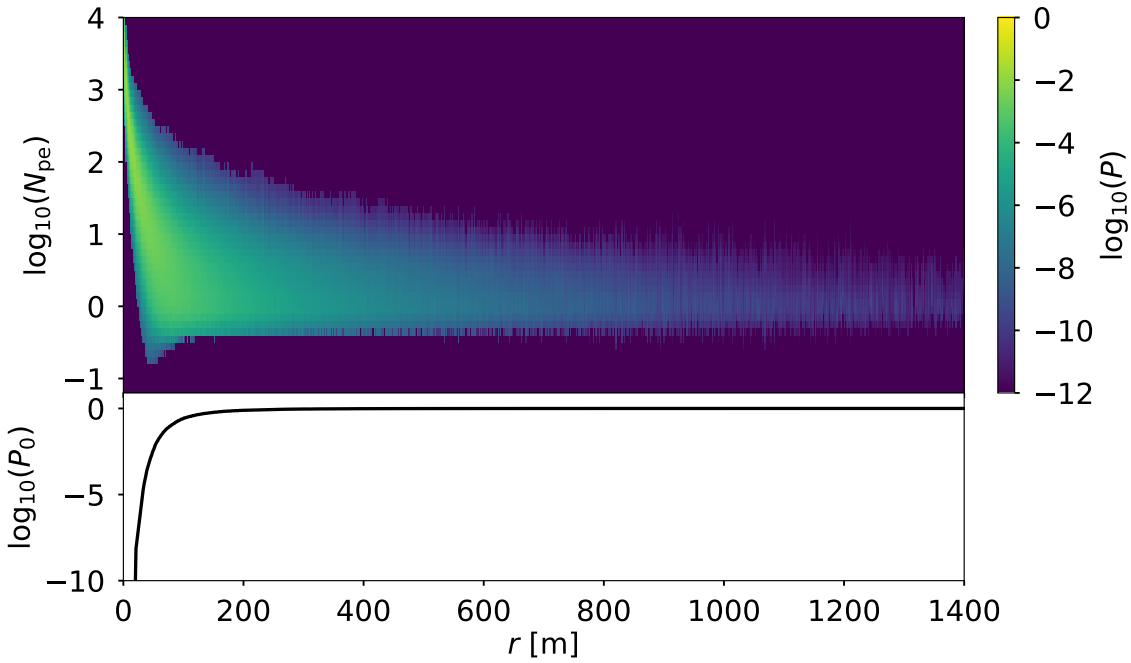


Figure 2: Monte Carlo generated template binned in $E = 7.1 - 8.0 \text{ TeV}$, $X_{\max} = 400 - 450 \text{ g/cm}^2$, and zenith angle $\theta = 0 - 19^\circ$. The probability P of measuring a specific number of photoelectrons for each distance r between the core and the tanks in the shower plane is plotted in the 2D histogram. The probability P_0 that no photoelectron is measured for a specific distance r is plotted in the bottom panel.

of the electronics in real operations. It is thereby possible to achieve slightly negative values for $\log(N_{\text{pe}})$. The bottom panel of Figure 2 shows the probability P_0 that no signal was measured in a tank at a distance r from the shower core in the shower plane, which is also used in the reconstruction to constrain the likelihood.

We implemented the model in the current SWGO standard reconstruction chain to reconstruct the energy and core position of the particle shower, where we measure the signal in each detector unit and fit this shower footprint against the probability functions of the templates. For the fit, we minimize the negative log-likelihood:

$$\log(L) = -2 \sum_i \log(P(\log_{10}(N_{\text{pe}})_i, r_i, X_{\max}, E | \theta, \phi)). \quad (1)$$

In this case, P is the individual tank probability that depends on the measured signal $\log_{10}(N_{\text{pe}})_i$, the distance r_i between the shower core and the tanks in the shower plane, the energy E and the maximum shower depth X_{\max} of the reconstructed particle shower. The incoming zenith and azimuth angles θ and ϕ were taken from the preliminary angular estimation that is applied beforehand using a plane fit. The starting values for the minimization of the core position are taken from a first rough core estimate with a center of mass estimation. The seeds for the E and X_{\max} are taken from lookup tables.

Figure 3 shows an example reconstruction of a gamma-ray shower. The true values of the primary gamma ray were $E_{\text{true}} = 6.8 \text{ TeV}$, $x_{\text{true}} = -2.2 \text{ m}$, $y_{\text{true}} = -92.7 \text{ m}$, $\theta_{\text{true}} = 13.5^\circ$ and $X_{\max,\text{true}} = 427 \text{ g/cm}^2$. The result for the core reconstruction is visualized in Figure 3a. Each

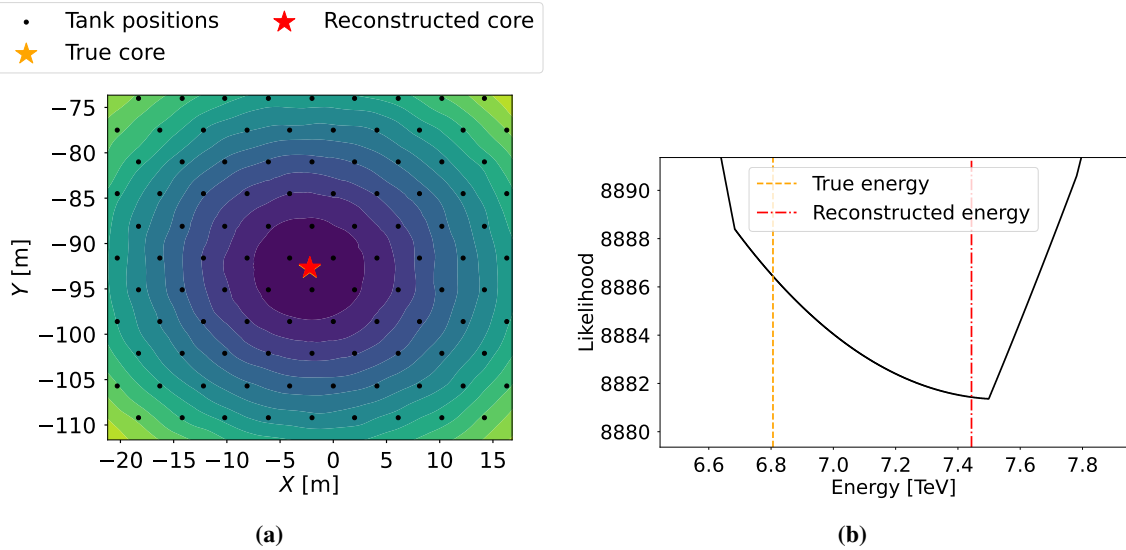


Figure 3: (a) Likelihood surface for the reconstruction of the shower core of an example event going from green (maximum) to purple (minimum). The different colored stars show the position of the reconstructed (red) and the true shower core (orange) on the array. (b) Likelihood values for the reconstruction of the energy of the same example event with the true (orange) and reconstructed (red) energies.

black dot represents the center of a tank, and the stars show the true core position (orange) and the reconstructed core position (red), respectively. Because the reconstructed core ($x_{\text{reco}} = -2.2$ m and $y_{\text{reco}} = -92.6$ m) of this event agrees excellently with the true core position, the orange star is barely visible. The visible contours ranging from green (maximum) to purple (minimum) denote the “likelihood surface” for the region around the reconstructed core, giving an estimate for the reconstruction uncertainty. In Figure 3b, we present the likelihood values in detail of and around the reconstructed energy $E_{\text{true}} = 7.4$ TeV. Again, the reconstructed value lies in the minimum of the likelihood values.

3. Energy estimation for one of the current test arrays

To validate the implementation of the method, we estimate the performance of the energy reconstruction of one of the current test arrays of SWGO. We use showers with a zenith angle below 45° whose true core fell directly on the array. In addition, some loose quality cuts were applied for the reconstruction. To examine the reconstruction performance, we show the reconstruction bias in Figure 4a and the energy resolution in Figure 4b. The used energy bias and resolution are defined as the mean and the RMS of the distribution of $\log_{10}(E_{\text{reco}}) - \log_{10}(E_{\text{true}})$. We compare the results for the test array with ones from HAWC [7] and ones that were estimated in the Southern Gamma-ray Survey Observatory (SGSO) white paper [6], which represents a first estimation of the future performance of SWGO. Both the energy bias as well as the energy resolution show promising results. At around 10 TeV an energy resolution of around 30% can be attained. Nevertheless, note that the reconstruction is still under development, and the final results can only be evaluated once the final array configuration of SWGO is fixed.

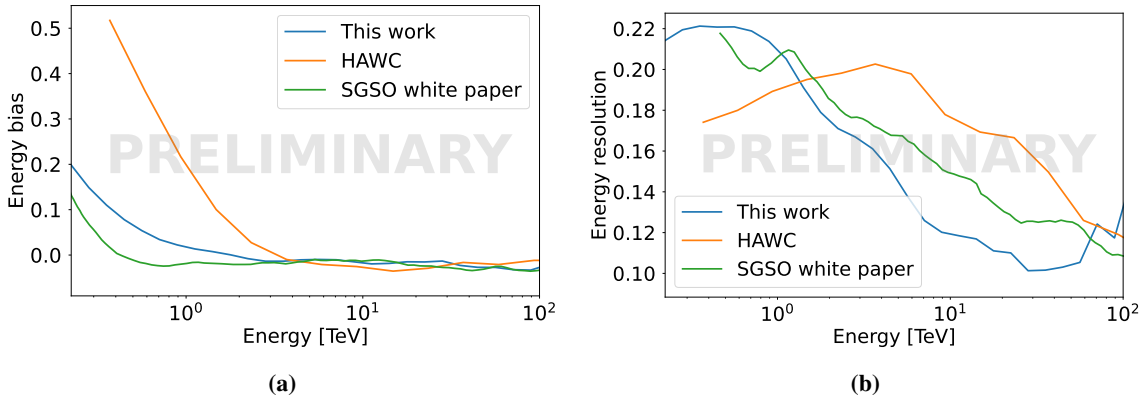


Figure 4: First results for the energy bias (a) and energy resolution (b) of an SWGO test configuration with results from HAWC [7] and the SGSO white paper [6] as a comparison. The bias and the resolution are calculated as mean and RMS of the distribution of $\log_{10}(E_{\text{reco}}) - \log_{10}(E_{\text{true}})$.

4. Summary and outlook

The standard reconstruction chain for the future SWGO is currently in development. One of the important steps within this chain is the implementation of a module for reconstructing particle energies. We applied a template-based method for the reconstruction of the energy and core position of gamma-induced particle showers for one of the current test arrays of SWGO. For this, we created a set of templates using Monte Carlo simulations. The observed lateral distribution function of a reconstructed shower is then fitted to the generated templates using a negative log-likelihood approach to find the best matching parameters for the core position and the energy. We validated the reconstruction by estimating the resolution of an example test array. The found energy bias and energy resolution of the investigated test array are very encouraging and similar to the performance estimated by the SGSO white paper [6]. We successfully implemented this method in the SWGO standard reconstruction framework offering a performance estimation of other SWGO test configurations. Once the final array configuration of SWGO is fixed, this method can be applied to estimate the final performance for the energy reconstruction of SWGO.

Acknowledgements

This work was supported by the Deutsche Forschungsgemeinschaft (DFG) under Grant No FU 1093/5-1 Optimierung des Designs von Wasser-Cherenkov-Detektoren für die Gammastrahlentomie. The SWGO Collaboration acknowledges the support from the agencies and organizations listed here: <https://www.swgo.org/SWGWiki/doku.php?id=acknowledgements>.

References

- [1] W. B. Atwood *et al.* [Fermi-LAT], “The Large Area Telescope on the Fermi Gamma-ray Space Telescope Mission,” *Astrophys. J.* **697** (2009), 1071–1102 doi:10.1088/0004-637X/697/2/1071 [arXiv:0902.1089 [astro-ph.IM]].

- [2] S. Funk, “Ground- and Space-Based Gamma-Ray Astronomy,” *Ann. Rev. Nucl. Part. Sci.* **65** (2015), 245-277 doi:10.1146/annurev-nucl-102014-022036 [arXiv:1508.05190 [astro-ph.HE]].
- [3] U. F. Katz, “Cherenkov light imaging in astroparticle physics,” *Nucl. Instrum. Meth. A* **952** (2020), 161654 doi:10.1016/j.nima.2018.11.113 [arXiv:1901.00146 [astro-ph.IM]].
- [4] A. U. Abeysekara *et al.* [historical and present HAWC], “The High-Altitude Water Cherenkov (HAWC) observatory in México: The primary detector,” *Nucl. Instrum. Meth. A* **1052** (2023), 168253 doi:10.1016/j.nima.2023.168253 [arXiv:2304.00730 [astro-ph.HE]].
- [5] A. Addazi *et al.* [LHAASO], “The Large High Altitude Air Shower Observatory (LHAASO) Science Book (2021 Edition),” *Chin. Phys. C* **46** (2022), 035001-035007 [arXiv:1905.02773 [astro-ph.HE]].
- [6] A. Albert, R. Alfaro, H. Ashkar, C. Alvarez, J. Alvarez, J. C. Arteaga-Velázquez, H. A. Ayala Solares, R. Arceo, J. A. Bellido and S. BenZvi, *et al.* “Science Case for a Wide Field-of-View Very-High-Energy Gamma-Ray Observatory in the Southern Hemisphere,” [arXiv:1902.08429 [astro-ph.HE]].
- [7] V. Joshi, J. Hinton, H. Schoorlemmer, R. López-Coto and R. Parsons, “A template-based γ -ray reconstruction method for air shower arrays,” *JCAP* **01** (2019), 012 doi:10.1088/1475-7516/2019/01/012 [arXiv:1809.07227 [astro-ph.IM]].
- [8] J. Hinton [SWGO], “The Southern Wide-field Gamma-ray Observatory: Status and Prospects,” *PoS ICRC2021* (2021), 023 doi:10.22323/1.395.0023 [arXiv:2111.13158 [astro-ph.IM]].
- [9] D. Heck, J. Knapp, J. N. Capdevielle, G. Schatz and T. Thouw, “CORSIKA: A Monte Carlo code to simulate extensive air showers,” *FZKA-6019*.
- [10] S. Agostinelli *et al.* [GEANT4], “GEANT4—a simulation toolkit,” *Nucl. Instrum. Meth. A* **506** (2003), 250-303 doi:10.1016/S0168-9002(03)01368-8

The SWGO Collaboration



P. Abreu^{1,2}, A. Albert³, R. Alfaro⁴, A. Alfonso⁵, C. Álvarez⁶, Q. An⁷, E. O. Angüner⁸, C. Arcaro⁹, R. Arceo⁶, S. Arias¹⁰, H. Arnaldi¹¹, P. Assis^{1,2}, H. A. Ayala Solares¹², A. Bakalova¹³, U. Barres de Almeida^{14,15}, I. Batkovic^{9,16}, J. Bazo¹⁷, J. Bellido^{18,19}, E. Belmont⁴, S. Y. BenZvi²⁰, A. Bernal²¹, W. Bian²², C. Bigongiari²³, E. Bottacini^{9,16}, P. Brogueira^{1,2}, T. Bulik²⁴, G. Busetto^{9,16}, K. S. Caballero-Mora⁶, P. Camarri^{25,26}, S. Campos²⁷, W. Cao⁷, Z. Cao⁷, Z. Cao²⁸, T. Capistrán²¹, M. Cardillo²³, E. Carquin²⁹, A. Carramíñana³⁰, C. Castromonte³¹, J. Chang²⁸, O. Chaparro³², S. Chen²², M. Chianese^{33,34}, A. Chiavassa^{35,36}, L. Chytka¹³, R. Colallillo^{33,34}, R. Conceição^{1,2}, G. Consolati^{37,38}, R. Cordero³⁹, P. J. Costa^{1,2}, J. Cotzomi⁴⁰, S. Dasso⁴¹, A. De Angelis^{9,16}, P. Desiati⁴², F. Di Pierro³⁶, G. Di Sciascio²⁵, J. C. Díaz Vélez⁴², C. Dib²⁹, B. Dingus³, J. Djupsland⁴³, C. Dobrigkeit⁴⁴, L. M. Domingues Mendes^{1,45}, T. Dorigo⁹, M. Doro^{9,16}, A. C. dos Reis¹⁴, M. Du Vernois⁴², M. Echiburú⁵, D. Elsaesser⁴⁶, K. Engel^{2,47}, T. Ergin⁴⁸, F. Espinoza⁵, K. Fang⁴², F. Farfán Carreras⁴⁹, A. Fazzi^{38,50}, C. Feng⁵¹, M. Feroci²³, N. Fraija²¹, S. Fraija²¹, A. Franceschini¹⁶, G. F. Franco¹⁴, S. Funk⁵², S. García¹⁰, J. A. García-González⁵³, F. Garfias²¹, G. Giacinti²², L. Gibilisco^{1,2}, J. Glombitzka⁵², H. Goksu⁴³, G. Gong⁵⁴, B. S. González^{1,2}, M. M. Gonzalez²¹, J. Goodman⁴⁷, M. Gu²⁸, F. Guarino^{33,34}, S. Gupta⁵⁵, F. Haist⁴³, H. Hakobyan²⁹, G. Han⁵⁶, P. Hansen⁵⁷, J. P. Harding³, J. Helo⁵, I. Herzog⁵⁸, H. d. Hidalgo⁶, J. Hinton⁴³, K. Hu⁵¹, D. Huang⁴⁷, P. Huentemeyer⁵⁹, F. Hueyotl-Zahuantitla⁶, A. Iriarte²¹, J. Isaković⁶⁰, A. Isolia⁶¹, V. Joshi⁵², J. Juryšek¹³, S. Kaci²², D. Kieda⁶², F. La Monaca²³, G. La Mura¹, R. G. Lang⁵², R. Laspiur²⁷, L. Lavitolá³⁴, J. Lee⁶³, F. Leitl⁵², L. Lessio²³, C. Li²⁸, J. Li⁷, K. Li²⁸, T. Li²², B. Liberti^{25,26}, S. Lin⁶⁴, D. Liu⁵¹, J. Liu²⁸, R. Liu⁶⁵, F. Longo^{66,67}, Y. Luo²², J. Lv⁶⁸, E. Macerata^{38,50}, K. Malone³, D. Mandat¹³, M. Manganaro⁶⁰, M. Mariani^{38,50}, A. Mariazzi⁵⁷, M. Mariotti^{9,16}, T. Marrodan⁴³, J. Martínez³², H. Martínez-Huerta⁶⁹, S. Medina⁵, D. Melo⁷⁰, L. F. Mendes², E. Meza⁷², D. Miceli⁹, S. Miozzo²⁵, A. Mitchell⁵², A. Molinario^{36,71}, O. G. Morales-Olivares⁶, E. Moreno⁴⁰, A. Morselli^{25,26}, E. Mossini^{38,50}, M. Mostafá¹², F. Muleri²³, F. Nardi^{9,16}, A. Negro^{35,36}, L. Nellen⁷³, V. Novotny¹³, E. Orlando^{66,67}, M. Osorio²¹, L. Otiniano⁷², M. Peresano^{35,36}, G. Piano²³, A. Pichel⁴¹, M. Pihet^{9,16}, M. Pimenta^{1,2}, E. Prandini^{9,16}, J. Qin⁷, E. Quispe^{72,74}, S. Rainò⁷⁵, E. Rangel²¹, A. Reisenegger⁵⁵, H. Ren⁴³, F. Reščić⁶⁰, B. Reville⁴³, C. D. Rho⁷⁶, M. Riquelme⁷⁷, G. Rodriguez Fernandez²⁵, Y. Roh⁶³, G. E. Romero⁴⁹, B. Rossi³⁴, A. C. Rovero⁴¹, E. Ruiz-Velasco⁴³, G. Salazar²⁷, J. Samanes⁷², F. Sanchez⁷⁰, A. Sandoval⁴, M. Santander⁷⁸, R. Santonico^{25,26}, G. L. P. Santos¹⁴, N. Saviano^{33,34}, M. Schneider⁴⁷, M. Schneider⁵², H. Schoorlemmer⁷⁹, J. Serna-Franco⁴, V. Serrano²⁷, A. Smith⁴⁷, Y. Son⁶³, O. Soto⁸⁰, R. W. Springer⁶², L. A. Stuani⁸¹, H. Sun⁵¹, R. Tang²², Z. Tang⁷, S. Tapia²⁹, M. Tavani²³, T. Terzić⁶⁰, K. Tollefson⁵⁸, B. Tomé^{1,2}, I. Torres³⁰, R. Torres-Escobedo²², G. C. Trinchero^{36,71}, R. Turner⁵⁹, P. Ulloa⁸⁰, L. Valore^{33,34}, C. van Eldik⁵², I. Vergara⁵⁷, A. Viana⁸², J. Víchá¹³, C. F. Vigorito^{35,36}, V. Vittorini²³, B. Wang⁵¹, J. Wang⁴³, L. Wang²⁸, X. Wang⁵⁹, X. Wang⁶⁵, X. Wang⁸³, Z. Wang²², M. Waqas^{33,34}, I. J. Watson⁶³, F. Werner⁴³, R. White⁴³, C. Wiebusch⁸⁴, E. J. Wilcox⁴⁷, F. Wohlleben⁴³, S. Wu²⁸, S. Xi²⁸, G. Xiao²⁸, L. Yang⁶⁴, R. Yang⁷, R. Yanyachi¹⁸, Z. Yao²⁸, D. Zavrtanik⁸⁵, H. Zhang²², H. Zhang⁶⁵, S. Zhang⁸⁶, X. Zhang²⁸, Y. Zhang⁶⁸, J. Zhao²⁸, L. Zhao⁷, H. Zhou²², C. Zhu⁵¹, P. Zhu⁸⁶, X. Zuo²⁸

POS (ICRC 2023) 593

¹ Laboratório de Instrumentação e Física Experimental de Partículas - LIP, Av. Prof. Gama Pinto, 2, 1649-003 Lisboa, Portugal

² Departamento de Física, Instituto Superior Técnico, Universidade de Lisboa, Av. Rovisco Pais 1, 1049-001 Lisboa, Portugal

³ Physics Division, Los Alamos National Laboratory, Los Alamos, NM, USA

⁴ Instituto de Física, Universidad Nacional Autónoma de México, Circuito de la Investigación científica, C.U., A. Postal 70-364, 04510 Cd. de México, México

⁵ Universidad de La Serena, Chile

⁶ Facultad de Ciencias en Física y Matemáticas, Universidad Autónoma de Chiapas, C. P. 29050, Tuxtla Gutiérrez, Chiapas, México

⁷ School of physical science, University of Science and Technology of China, 96 Jinzhai Road, Hefei, Anhui 230026, China

⁸ TÜBİTAK Research Institute for Fundamental Sciences, 41470 Gebze, Turkey

⁹ INFN - Sezione di Padova, I-35131, Padova, Italy

¹⁰ Universidad Nacional de San Antonio Abad del Cusco, Av. de la Cultura, Nro. 733, Cusco - Perú

¹¹ Centro Atómico Bariloche (CNEA-CONICET-IB/UNCuyo), Av. E. Bustillo 9500, (8400) San Carlos de Bariloche, Rio Negro, Argentina

¹² Department of Physics, Pennsylvania State University, University Park, PA, USA

¹³ Institute of Physics of the Czech Academy of Sciences, Prague, Czech Republic

¹⁴ Centro Brasileiro de Pesquisas Físicas (CBPF), Rua Dr. Xavier Sigaud 150, 22290-180 Rio de Janeiro, Brasil

¹⁵ Universidade de São Paulo, Instituto de Astronomia, Geofísica e Ciências Atmosféricas, Departamento de Astronomia, Rua do Matão 1226, 05508-090 São Paulo, Brasil

¹⁶ Università di Padova, I-35131, Padova, Italy

¹⁷ Pontificia Universidad Católica del Perú, Av. Universitaria 1801, San Miguel, 15088, Lima, Perú

¹⁸ Universidad Nacional de San Agustín de Arequipa, Santa Catalina Nro. 117. Arequipa

¹⁹ University of Adelaide, Adelaide, S.A., Australia

²⁰ Department of Physics and Astronomy, University of Rochester, Rochester, NY, USA

²¹ Instituto de Astronomía, Universidad Nacional Autónoma de México, Circuito Exterior, C.U., A. Postal 70-264, 04510 Cd. de México, México

²² Tsung-Dao Lee Institute and School of Physics and Astronomy, Shanghai Jiao Tong University, 520 Shengrong Road, Shanghai 201210, China

- ²³ Istituto Nazionale Di Astrofisica (INAF), Roma, Italy
²⁴ Astronomical Observatory Warsaw University, 00-478 Warsaw, Poland
²⁵ INFN, Roma Tor Vergata, Italy
²⁶ Department of Physics, University of Roma Tor Vergata, Viale della Ricerca Scientifica 1, I-00133 Roma, Italy
²⁷ Facultad de Ciencias Exactas, Universidad Nacional de Salta, Avda. Bolivia 5150, A4408FVY, Salta, Argentina
²⁸ Institute of High Energy Physics, Chinese Academy of Science, 19B Yuquan Road, Shijingshan District, Beijing 100049, China
²⁹ CCTVal, Universidad Tecnica Federico Santa Maria, Chile
³⁰ Instituto Nacional de Astrofísica, Óptica y Electrónica, Puebla, Mexico
³¹ Universidad Nacional de Ingeniería, Av. Túpac Amaru 210 - Rímac. Apartado 1301, Lima Perú
³² Centro de Investigación en Computación, Instituto Politécnico Nacional, Ciudad de México, Mexico
³³ Università di Napoli "Federico II", Dipartimento di Fisica "Ettore Pancini", Napoli, Italy
³⁴ INFN, Sezione di Napoli, Napoli, Italy
³⁵ Università degli Studi di Torino, I-10125 Torino, Italy
³⁶ INFN, Sezione di Torino, Torino, Italy
³⁷ Politecnico di Milano, Dipartimento di Scienze e Tecnologie Aeroespaziali, Milano, Italy
³⁸ INFN, sezione di Milano, Milano, Italy
³⁹ Departamento de Física, Universidad de Santiago de Chile, Chile
⁴⁰ Facultad de Ciencias Físico Matemáticas, Benemérita Universidad Autónoma de Puebla, Av. San Claudio y 18 Sur, Ciudad Universitaria 72570, Puebla, Mexico
⁴¹ Instituto de Astronomía y Física del Espacio (IAFE (CONICET-UBA)), Ciudad Universitaria, CABA, Argentina
⁴² Department of Physics, University of Wisconsin-Madison, Madison, WI, USA
⁴³ Max-Planck-Institut für Kernphysik, Saupfercheckweg 1, 69117 Heidelberg, Germany
⁴⁴ Departamento de Raios Cósmicos e Cronología, Instituto de Física "Gleb Wataghin", Universidade Estadual de Campinas, C.P. 6165, 13083-970 Campinas, Brasil
⁴⁵ Centro Federal de Educação Tecnológica Celso Suckow da Fonseca (CEFET), Rio de Janeiro, Brasil
⁴⁶ Technische Universität Dortmund, D-44221 Dortmund, Germany
⁴⁷ Department of Physics, University of Maryland, College Park, MD, USA
⁴⁸ Middle East Technical University, Northern Cyprus Campus, 99738 Kalkanli via Mersin 10, Turkey
⁴⁹ Instituto Argentino de Radioastronomía (CONICET, CIC, UNLP), Camino Gral. Belgrano Km 40, Berazategui, Argentina
⁵⁰ Politecnico di Milano, Dipartimento di Energia, Milano, Italy
⁵¹ Key Laboratory of Particle Physics and Particle Irradiation (MOE), Institute of Frontier and Interdisciplinary Science, Shandong University, Qingdao, Shandong 266237, China
⁵² Friedrich-Alexander-Universität Erlangen-Nürnberg, Erlangen Centre for Astroparticle Physics, Nikolaus-Fiebiger-Str. 2, D 91058 Erlangen, Germany
⁵³ Tecnológico de Monterrey, Escuela de Ingeniería y Ciencias, Ave. Eugenio Garza Sada 2501, Monterrey, N.L., Mexico, 64849
⁵⁴ Dept. of Engineering Physics, Tsinghua University, 1 Tsinghua Yuan, Haidian District, Beijing 100084, China
⁵⁵ Universidad Metropolitana de Ciencias de la Educación (UMCE), Chile
⁵⁶ School of Mechanical Engineering and Electronic Information, China University of Geosciences, Wuhan, Hubei 430074, China
⁵⁷ IFLP, Universidad Nacional de La Plata and CONICET, La Plata, Argentina
⁵⁸ Department of Physics and Astronomy, Michigan State University, East Lansing, MI, USA
⁵⁹ Michigan Technological University, Houghton, Michigan, 49931, USA
⁶⁰ University of Rijeka, Faculty of Physics, 51000 Rijeka, Croatia
⁶¹ Università di Catania, Catania, Italy
⁶² Department of Physics and Astronomy, University of Utah, Salt Lake City, UT, USA
⁶³ University of Seoul, Seoul, Rep. of Korea
⁶⁴ School of Physics and Astronomy, Sun Yat-sen University, Zhuhai, Guangdong 519082, China
⁶⁵ School of Astronomy and Space Science, Nanjing University, Xianlin Avenue 163, Qixia District, Nanjing, Jiangsu 210023, China
⁶⁶ Dipartimento di Fisica, Università degli Studi di Trieste, Trieste, Italy
⁶⁷ INFN - Sezione di Trieste, via Valerio 2, I - 34149, Trieste, Italy
⁶⁸ Aerospace Information Research Institute, Chinese Academy of Science, 9 Dengzhuang South Road, Haidian District, Beijing 100094, China
⁶⁹ Departamento de Física y Matemáticas, Universidad de Monterrey, Av. Morones Prieto 4500, 66238, San Pedro Garza García NL, México
⁷⁰ Instituto de Tecnologías en Detección y Astropartículas (CNEA, CONICET, UNSAM), Buenos Aires, Argentina
⁷¹ Instituto Nazionale Di Astrofisica (INAF), Torino, Italy
⁷² Comisión Nacional de Investigación y Desarrollo Aeroespacial, Perú
⁷³ Instituto de Ciencias Nucleares, Universidad Nacional Autónoma de México, Circuito Exterior, C.U., A. Postal 70-543, 04510 Cd. de México, México
⁷⁴ Universidad Nacional de Moquegua, None
⁷⁵ Università degli Studi di Bari Aldo Moro, Italy
⁷⁶ Department of Physics, Sungkyunkwan University, Suwon, South Korea

⁷⁷ Universidad de Chile, Chile

⁷⁸ Department of Physics and Astronomy, University of Alabama, Tuscaloosa, Alabama, 35487, USA

⁷⁹ IMAPP, Radboud University Nijmegen, Nijmegen, The Netherlands

⁸⁰ Unidade Acadêmica de Física, Universidade Federal de Campina Grande, Av. Aprígio Veloso 882, CY2, 58.429-900 Campina Grande, Brasil

⁸¹ Instituto de Física de São Carlos, Universidade de São Paulo, Av. Trabalhador São-carlense 400, São Carlos, Brasil

⁸² School of Integrated Circuit, Ludong University, 186 Hongqi Middle Road, Zhifu District, Yantai, Shandong, China

⁸³ III. Physics Institute A, RWTH Aachen University, Templergraben 56, D-52062 Aachen, Germany

⁸⁴ Center for Astrophysics and Cosmology (CAC), University of Nova Gorica, Nova Gorica, Slovenia

⁸⁵ College of Engineering, Hebei Normal University, 20 South Second Ring East Road, Shijiazhuang, Hebei, China

⁸⁶ School of mechanical engineering, University of Science and Technology Beijing, 30 Xueyuan Road, Haidian District, Beijing 100083, China